Kuwait J. Sci. **47 (2)** pp. 34-40, 2020

ازدياد المغنطة في المركبات الحديدية السيراميكية $Bi_{0.94}Sm_{0.06}FeO_3$ المحقونة بالعنصر Y

منصور محمد الحاج
قسم الفيزياء، جامعة مؤتة، مؤتة، الكرك، الأردن

الملخص

وجد أن التركيب البلوري لجميع المركبات المدروسة هو المسطح المعيني المشوّه. تم استخلاص معاملات النظام الشبكي من حيود الأشعة السينية. أيّدت الإمتصاصات الطيفية الجزيئية تحت الحمراء التركيب البلوري لهذه المواد. وُجد أيضاً أنّ المواد SmY00 و SmY02 هي ذات خصائص فرومغناطيسية ضعيفة ومتشابهة، بينما أظهرت المادة SmY06 فرومغناطيسية مدعّمة. تم قياس درجة حرارة التحوّل المغناطيسي للمواد بحدود 350 – 340 °C.

Enhanced magnetization in Y substituted $Bi_{0.94}Sm_{0.06}FeO_3$ multiferroic ceramics

Mansour M. Al-Haj

Dept. of Physics, Mutah University, Mutah, Al-Karak, Jordan

Corresponding author: mansour@mutah.edu.jo

Abstract

The compounds $Bi_{0.94}Sm_{0.06}FeO_3$, $Bi_{0.92}Sm_{0.06}Y_{0.02}FeO_3$, $Bi_{0.90}Sm_{0.06}Y_{0.04}FeO_3$, and $Bi_{0.88}Sm_{0.06}Y_{0.06}FeO_3$ were found to have the rhombohedral perovskite-like structure. The structural parameters were extracted from X-ray diffraction data. The Fourier transform infrared spectroscopy revealed three absorption bands in the wavenumber range 400 – 2000 cm^{-1}. The $Bi_{0.94}Sm_{0.06}FeO_3$ and $Bi_{0.92}Sm_{0.06}Y_{0.02}FeO_3$ compounds were found to have similar weak ferromagnetic behaviors, whereas the ferromagnetism of the $Bi_{0.88}Sm_{0.06}Y_{0.06}FeO_3$ compound was found to be soft and substantially enhanced. The magnetic transition temperatures were in the range 340 – 350 °C.

Keywords: Impurity; magnetization; spectroscopy; transition temperature; X-ray diffraction.

1. Introduction

The inorganic compound $BiFeO_3$ (BFO) is a fascinating multiferroic material that has interested researchers for the last few decades. The structure of BFO can be described as a rhombohedrally distorted perovskite with the space group R3c (Kubel & Schmid, 1990). This material undergoes an antiferromagnetic-paramagnetic transition at about 370 °C, and a ferroelectric-paraelectric transition occurs at about 830 °C. Researchers seek to tailor the structural, optical, magnetic, dielectric, and electrical properties for possible applications in the fields of data storage, spintronics, photocatalysis, photovoltaic, and antibacterial activity (Ravichandran *et al.*, 2018).

Current research includes the effect of calcination conditions on performance (Maleki *et al.*, 2018), the chemical synthesis of nanostructured materials (Wang *et al.*, 2018), and the effect of one ion doping such as Mo (Murtaza *et al.*, 2018), Eu (Mumtaz *et al.*, 2018), Nd (Maleki *et al.*, 2018), Sr (Shisode *et al.*, 2018), and Ba (Shisode *et al.*, 2018). Other recent studies investigate the effect of two ion doping such as La-Gd (Bozgeyik *et al.*, 2018), La-Ni (Sharma *et al.*, 2018), Gd-Sr (Al-Haj, 2010), and Cu-Ti (Rafiq *et al.*, 2018). More studies focused on topics such as structural transformation by means of *ab-initio* calculations (Graf *et al.*, 2018); photocatalytic performance of $BiFeO_3$ in the degradation of methylene blue dye under visible light irradiation (Nadeem *et al.*, 2018; Maleki, 2018); theoretical magnetocaloric calculations (Amirov *et al.*, 2018); and thermal stability (Meera *et al.*, 2019). Various techniques have explored complex impedance spectroscopy (Hussain *et al.*, 2018), electron spin resonance spectroscopy (Biswal *et al.*, 2018), Mössbauer spectroscopy (Amirov *et al.*, 2018), electron energy-loss spectroscopy (Wang *et al.*, 2019), piezoresponse force microscopy (Wang *et al.*, 2019), and in-situ energy-dispersive X-ray diffraction (Wassel *et al.*, 2019). All these works have significantly contributed to the knowledge and understanding of BFO. However, despite such progress, there are still controversies regarding phase transformation and the appearance of weak ferromagnetism in ion-substituted BFO. Thus, more research is still needed to develop a complete understanding of this material.

We investigate the multiferroic compounds $Bi_{0.94}Sm_{0.06}FeO_3$, $Bi_{0.92}Sm_{0.06}Y_{0.02}FeO_3$, $Bi_{0.90}Sm_{0.06}Y_{0.04}FeO_3$, and $Bi_{0.88}Sm_{0.06}Y_{0.06}FeO_3$ through various experimental methods. Throughout this paper, they will be referred to as SmY00, SmY02, SmY04, and SmY06, respectively.

2. Experimental methods

The compounds were prepared by the usual solid state reaction method. Stoichiometric amounts of pure oxides of Bi_2O_3, Y_2O_3, Sm_2O_3, and Fe_2O_3 were well mixed and ground in an agate mortar and pestle. The resulting mixtures were pre-calcined at 830 °C in a conventional furnace for 60 min. After the calcination process, the mixtures were left to slowly cool to room temperature, at which time they were ground, and calcined again

at 830 °C for another 60 min. Then the mixtures were cooled to room temperature and ground to obtain a fine powder. X-ray diffraction (XRD) patterns were recorded by a Seifert 3003TT powder diffractometer using the CuK_{α} radiation. The Fourier transform infrared (FTIR) spectra of the samples were collected by a JASCO E300 spectrometer in the wavenumber range 400 - 2000 cm^{-1}. Since potassium bromide (KBr) does not show any absorption spectrum in the IR region, a minute quantity of each powder was mixed with a substantial quantity of KBr and then pressed into thin pellets (thickness < 0.5 mm) for FTIR spectra collection. The magnetic hysteresis loops were recorded by a conventional vibrating sample magnetometer (VSM) calibrated with a standard nickel sphere. The magnetic transition temperature was measured by a Mettler differential scanning calorimeter (DSC) with a maximum operating temperature of 450 °C.

3. Results and discussion

Figures 1(a-d) show the XRD patterns of the SmY00, SmY02, SmY04, and SmY06 compounds. The reflection peaks in these patterns were indexed according to the $BiFeO_3$ diffraction pattern (PDF #86-1518), confirming the rhombohedral perovskite-like structure with space group R3c. However, small traces of the parasitic impurity phases, $Bi_2Fe_4O_9$ and $Bi_{25}FeO_{40}$, which roughly do not exceed a mass percentage of 5%, were seen. These are the inevitable impurity phases that were reported to emerge during the synthesis of related ion-substituted BFO compounds (Al-Haj, 2012; Al-Haj, 2010), and are formed due to the volatilization of Bi. In general, the role of Y^{3+} in stabilizing the crystal structure of the compounds and in suppressing the formation of the impurity phase can be recognized in the XRD patterns (in particular, SmY04).

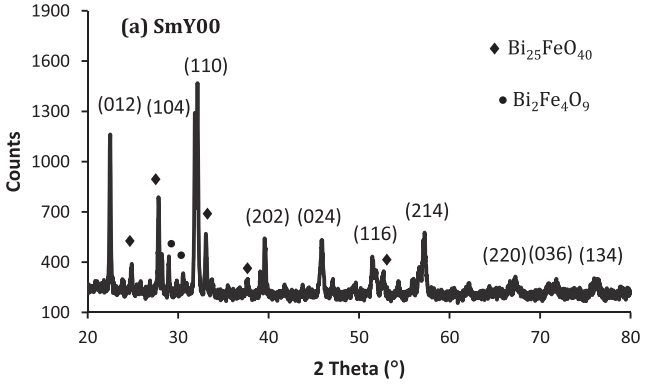

Fig. 1(a). The XRD pattern of SmY00.

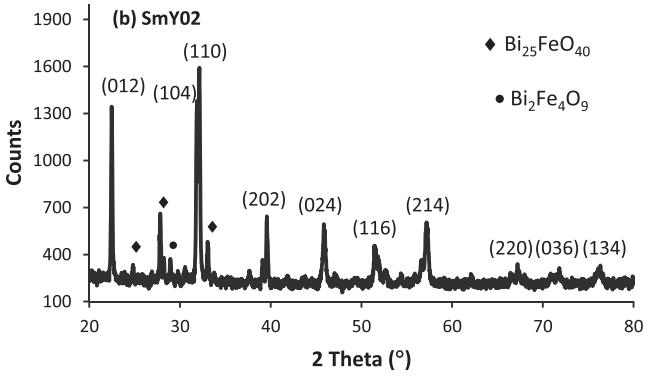

Fig. 1(b). The XRD pattern of SmY02.

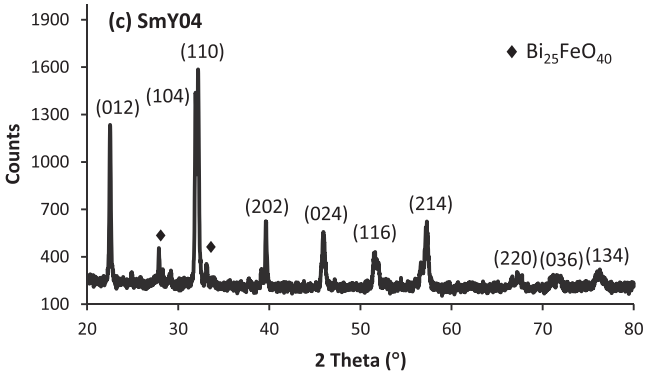

Fig. 1(c). The XRD pattern of SmY04.

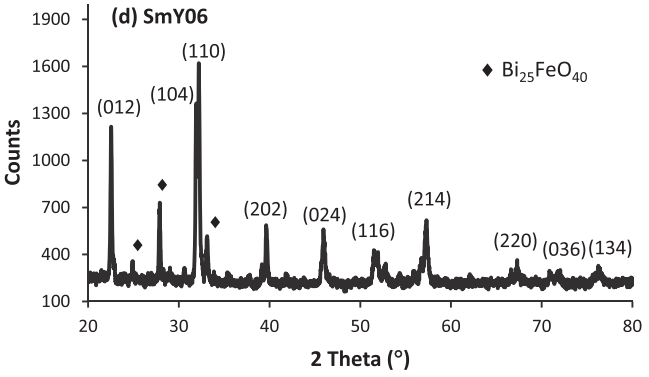

Fig. 1(d). The XRD pattern of SmY06.

In order to extract accurate values of the structural parameters of the studied materials, we carried out a least-squares refinement calculation of the XRD data using the UNITCELL program (Holland & Redfern, 1997). The obtained values of the hexagonal unit cell lattice parameters *a* and *c* are in very good agreement with other reported values in the literature, shown in Figure 2 with their fitting lines. Since the radius of Y^{3+} = 0.9 Å < radius of Bi^{3+} = 1.03 Å, the expected trend of the lattice parameters is to decrease slightly with the Y^{3+} content (see Figure 2). In conclusion, the substituting process has caused distortion in the rhombohedral unit cell which manifests itself in a change in the Bi/Fe-O bond length and the Bi-O-Fe bond angle.

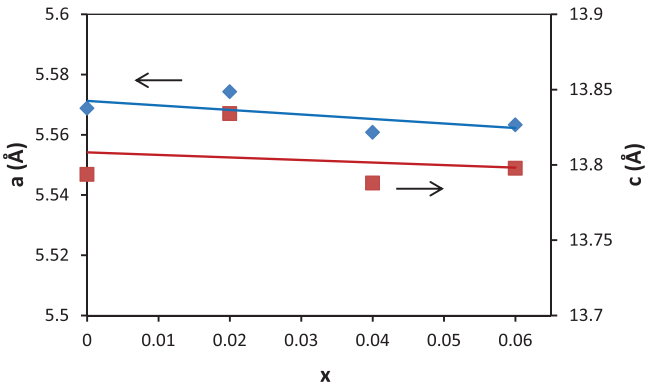

Fig. 2. The values of the lattice parameters and their fitting lines.

Another important point considered is the existence of traces of the soft ferrite phase Fe_3O_4 (PDF #87-2334), which has a strong reflection peak at $2\theta = 35.4°$ in its XRD pattern. In fact, a careful search-match process did not show any traces of this magnetic phase.

Figures 3(a-d) show the FTIR spectra for the SmY00, SmY02, SmY04, and SmY06 compounds in the wavenumber range 400 - 2000 cm^{-1}. Three distinct absorption peaks can be seen in each spectrum. The peaks at 444 - 447 cm^{-1} correspond to the O-Fe-O bending vibrations. The peaks at 550 - 555 cm^{-1} correspond to the Fe-O stretching vibrations, while the absorption peaks at 820 - 830 cm^{-1} will be addressed shortly. The peaks obtained for the bending and stretching vibrations of the FeO_6 octahedral unit of the rhombohedral cell are in excellent agreement with previous research outcomes. This assures the respectable quality of our samples. On the other hand, some researchers attributed the origin of the peaks at 820 – 830 cm^{-1} to ionic groups from the raw materials, which is unsatisfactory. These peaks are more likely related to the impurities in the samples. As seen in Figure 3, the third peak in each spectrum becomes weaker as the Y^{3+} content is increased, confirming our earlier conclusion regarding the general role played by Y^{3+} in suppressing impurity phases.

The room temperature magnetic hysteresis loops of the studied compounds are shown in Figures 4(a, b), and the obtained values of the remnant magnetization M_r and coercive field H_c are listed in Table 1. The data show that the compounds SmY00 and SmY02 (Figure 4a) exhibit weak ferromagnetism with unsaturated magnetization and open hysteresis loop with nearly equal magnetic parameters. (In Figure 4a, the overlap of the two loops in the first quadrant is due to small fluctuations in the magnetic field at the start of measurement, but that does not affect the magnetic parameters.) The SmY04 and SmY06 compounds exhibit enhanced saturated soft ferromagnetic behavior (Figure 4b). Since the Sm^{3+} content in all the compounds is the same, the magnetization change is mainly due to Y^{3+}. Some factors that may change the magnetization of ion-substituted BFO compounds are: (1) The soft ferrite magnetic phase has already been excluded from our samples; the impurity phase $Bi_2Fe_4O_9$ is diamagnetic at room temperature, and the weak ferromagnetism of the impurity phase $Bi_{25}FeO_{40}$ at room temperature (Kumari & Khare, 2017) is insufficient to alter the magnetization of our samples. All these together exclude any contribution to the magnetization from impurity phases. (2) Table 1 shows that the M_r value of SmY02 is 0.0086 emu/g, and that of SmY04 is 0.018 emu/g, which is greater by a factor of about 2. The M_r value of SmY06 increased by a factor of about 5 relative to that of SmY04. Such an enhancement in magnetization could be caused by the suppression of the helical spin structure of ion-substituted BFO due to lattice distortion. (3) Chemical inhomogeneity is considered a cause for magnetization enhancement in the research samples because the Bi site in BFO was replaced by two different ions: Sm^{3+} and Y^{3+}. (4) Since the oxidation states of Bi^{3+} and Y^{3+} are the same, there is no influence of the oxidation state on magnetization, and consequently, the role of oxygen vacancies is ruled out as well. However, to be sure of this point, XPS studies should be done.

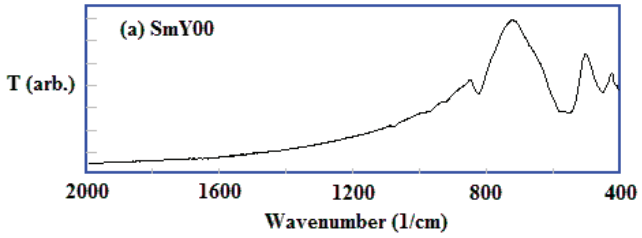

Fig. 3(a). The FTIR spectrum of SmY00.

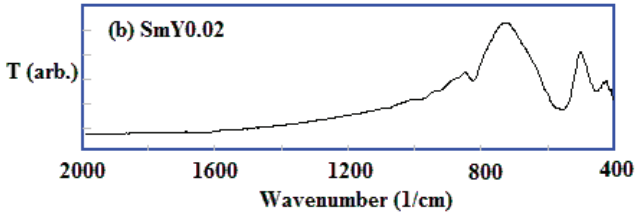

Fig. 3(b). The FTIR spectrum of SmY02.

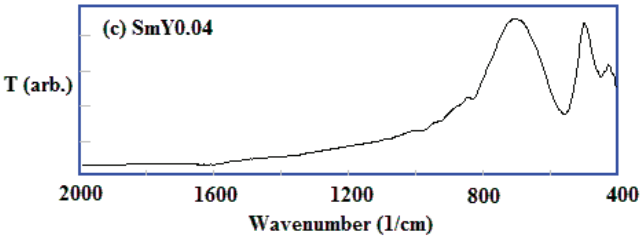

Fig. 3(c). The FTIR spectrum of SmY04.

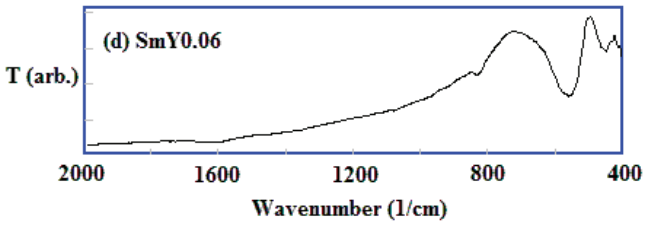

Fig. 3(d). The FTIR spectrum of SmY06.

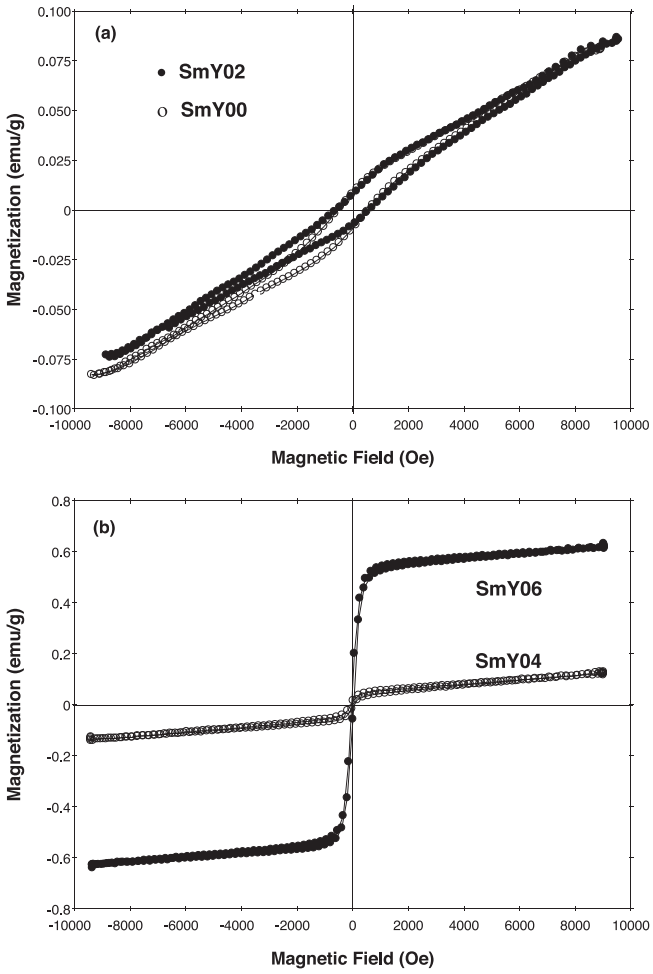

Fig. 4. The magnetic hysteresis loops of the studied compounds.

Table 1. The M_r and H_c values of the studied ceramics

Compound	M_r (emu/g)	H_c (Oe)
SmY00	0.0093	500
SmY02	0.0086	575
SmY04	0.018	90
SmY06	0.088	90

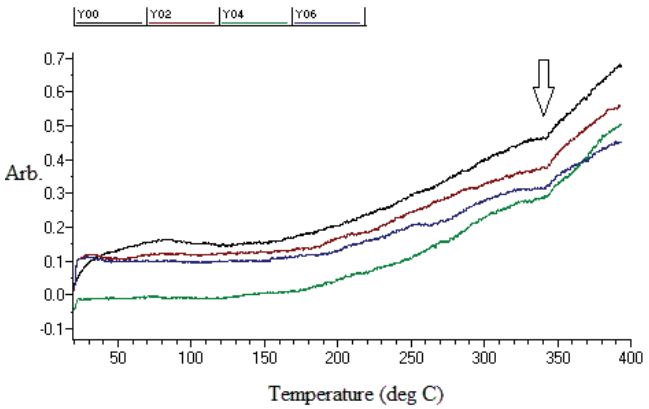

Fig. 5. The DSC scans of the studied compounds.

One possible use of DSC is to identify the magnetic transition temperature T_N, which is characterized by a weak endothermic peak on the DSC scan. In practice, such a peak is hard to detect because it could overlap with other noisy signals, especially if the baseline fluctuates with temperature. Nonetheless, by properly choosing the sample mass and heating rate, the transition could be detected. Figure 5 shows the DSC scans of the studied compounds that were obtained after several unsuccessful trials. As seen in this figure, the magnetic transition signal is very weak, and this is the reason why DSC is less commonly employed for these types of measurement. The magnetic transition temperatures of all the samples were in the range of 340 – 350 °C, which seems reasonable.

4. Conclusions

A comparative study was carried out of the structural and magnetic properties of the compounds SmY00, SmY02, SmY04, and SmY06, prepared by the solid state reaction method. They were analyzed by structural, spectroscopic, magnetic, and thermal techniques. It was found that the compounds SmY00 and SmY02 show similar weak ferromagnetic behaviors, while the ferromagnetism of SmY06 is substantially enhanced. The magnetic transition temperatures were obtained by thermal calorimetry.

References

Al-Haj, M. (2010). Preparation and characterization of $Bi_{0.9}M_{0.05}N_{0.05}FeO_3$ (M = Sm, Gd; N = Sr, Y) polycrystalline multiferroic compounds. Crystal Research and Technology, **45**(11): 1145-1148.

Al-Haj, M. (2010). X-ray diffraction and magnetization studies of $BiFeO_3$ multiferroic compounds substituted by Sm^{3+}, Gd^{3+}, Ca^{2+}. Crystal Research and Technology, **45**(1): 89-93.

Al-Haj, M. (2012). Structural and magnetic characterization of $Bi_{0.9}Ca_{0.1}Fe_{0.98}X_{0.02}O_3$ (X = Mg, Al, Ti, V) polycrystalline multiferroic compounds. Turkish Journal of Physics, **36**(3): 415-421.

Amirov, A.A., Guseynov, M.M., Yusupov, D.M., Abdulkadirova, N.Z., Chaudhary, Y.A., *et al.,* (2018). X-ray diffraction and Mössbauer studies of the structural features of $BiFe_{1-x}Zn_xO_3$ multiferroics. Journal of Surface Investigation: X-Ray, Synchrotron and Neutron Techniques, **12**(4): 732-736.

Amirov, A.A., Makoed, I.I., Chaudhari, Y.A., Bendre, S.T., Yusupov, D.M., *et al.,* (2018). Magnetcaloric effect in $BiFe_{1-x}Zn_xO_3$ multiferroics. Journal of Superconductivity and Novel Magnetism, **31**: 3283-3288.

Biswal, M.R., Nanda, J., Mishra, N.C., Acharya, S.S., Mishra, D.K., *et al.,* (2018). Magnetism in $BiFe_{1-x}Ni_xO_3$: studied through electron spin resonance spectroscopy. Journal of Materials Science: Materials in Electronics, **29**: 20595-20602.

Bozgeyik, M.S., Katiyar, R.K. & Katiyar, R.S. (2018). Improved magnetic properties of bismuth ferrite ceramics by La and Gd co-substitution. Journal of Electroceramics, **40**: 247-256.

Graf, M.E., Napoli, S.D., Barral, M.A., Medina, L.M., Negri, R.M., *et al.,* (2018). Rhombohedral R3c to orthorhombic Pnma phase transition induced by Y-doping in $BiFeO_3$. Journal of Physics: Condensed Matter, **30**: 285701 (8pp).

Holland, T. & Redfern, S. (1997). UNITCELL refinement from powder diffraction data: the use of regression diagnostics. Mineralogical Magazine, **61**: 65-77.

Hussain, S., Khan, F.A., Hasanain, S.K., Awan, S.U. & Raza, S.A. (2018). Investigation of dielectric and complex impedance spectroscopic studies of $Bi_{1-x}Ba_xFeO_3$ ($0 \leq x \leq 0.30$) system. Journal of Materials Science: Materials in Electronics, **29**: 8327-8337.

Kubel, F. & Schmid, H. (1990). Structure of a ferroelectric and ferroelastic monodomain crystal of the perovskite $BiFeO_3$. Acta Crystallographica, **B46**(6): 698-702.

Kumari, P. & Khare, N. (2017). Structural, optical and magnetic properties of $Bi_{25}FeO_{40}$ nanoparticles synthesized by hydrothermal method. In: Jain, V., Rattan, S. & Verma, A. (Eds.). Recent Trends in Materials and Devices. Springer Proceedings in Physics, **178**: 139-143.

Maleki, H. (2018). Photocatalytic activity and magnetic enhancements by addition of lanthanum into the $BiFeO_3$ structure and the effect of synthesis method. Journal of Materials Science: Materials in Electronics, **29**: 11862-11869.

Maleki, H., Haselpour, M. & Fathi, R. (2018). The effect of calcination conditions on structural and magnetic behavior of bismuth ferrite synthesized by co-precipitation method. Journal of Materials Science: Materials in Electronics, **28**: 4320-4326.

Maleki, H., Zare, S. & Fathi, R. (2018). Effect of Nd substitution on properties of multiferroic bismuth ferrite synthesized by sol-gel auto combustion method. Journal of Superconductivity and Novel Magnetism, **31**: 2539-2545.

Meera, A.V., Ganesan, R. & Gnanasekaran, T. (2019). Studies on the thermal stability of $BiFeO_3$ and the phase diagram of Bi-Fe-O system. Journal of Alloys and Compounds, **790**: 1108-1118.

Mumtaz, F., Jaffari, G.H. & Shah, S.I. (2018). Peculiar magnetism in Eu substituted $BiFeO_3$ and its correlation with local structure. Journal of Physics: Condensed Matter, **30**: 435802 (17pp).

Murtaza, T., Salmani, I.A., Ali, J. & Khan, M.S. (2018). Effect of Mo doping at the B site on structural and electrical properties of multiferroic $BiFeO_3$. Journal of Superconductivity and Novel Magnetism, **31**: 1955-1959.

Nadeem, M., Khan, W., Khan, S., Shoeb, M., Husain, S., *et al.,* (2018). Significant enhancement in photocatalytic performance of Ni doped $BiFeO_3$ nanoparticles. Materials Research Express, **5**: 065506.

Rafiq, M.A., Muhammad, Q.K., Nasir, S., Amin, U., Maqbool, A., *et al.,* (2018). Structure, infra-red, dielectric properties and conduction mechanism of Ti and Cu-Ti co-doped bismuth ferrite ($BiFeO_3$): a comparison study. Applied Physics A, **124**: 748.

Ravichandran, A.T., Srinivas, J., Manikandan, A. & Baykal, A. (2018). Enhanced magneto-optical and antibacterial studies of $Bi_{1-x}Mg_xFeO_3$ ($0.0 \leq x \leq 0.15$) nanoparticles. Journal of Superconductivity and Novel Magnetism, **32**: 1663-1670.

Sharma, J., Hamid, B., Kumar, A. & Srivastava, A.K.

(2018). Investigation of structural and dielectric properties of La-Ni doped bismuth nano ferrite. Journal of Materials Science: Materials in Electronics, **29**: 1107-1117.

Shisode, M.V., Humbe, A.V., Kharat, P.B. & Jadhav, K.M. (2018). Influence of Ba^{2+} on opto-electric properties of nanocrystalline $BiFeO_3$ multiferroic. Journal of Electronic Materials, **48**: 358-367.

Shisode, M.V., Kounsalye, J.S., Humbe, A.V., Kambale, R.C. & Jadhav, K.M. (2018). Investigations of magnetic and ferroelectric properties of multiferroic Sr-doped bismuth ferrite. Applied Physics A, **124**: 603.

Wang, N., Li, Y., Wang, F.L., Zhou, S.D., Zhu, L., *et al.,* (2019). Structure, magnetic and ferroelectric properties of Sm and Sc doped $BiFeO_3$ polycrystalline ceramics. Journal of Alloys and Compounds, **789**: 894-903.

Wang, S., Xu, H.D., Cai, J., Wang, Y.P., Tao, H.L., *et al.,* (2019). Electronic structure of multiferroic $BiFeO_3$: Electron energy-loss spectroscopy and first-principles study. Micron, **120**: 43-47.

Wang, T., Song, S.H., Wang, X.L., Chen, J.J. & Tan, M.L. (2018). Chemical substitution-induced structure transition and enhanced magnetic and optical properties of sol-gel synthesized multiferroic $BiFeO_3$ nanoparticles. Journal Sol-Gel Science and Technology, **85**: 356-368.

Wassel, M.A., Pérez-Maqueda, L.A., Gil-Gonzalez, E., Charalambous, H., Perejon, A., *et al.,* (2019). Anisotropic lattice expansion determined during flash sintering of $BiFeO_3$ by in-situ energy-dispersive X-ray diffraction. Scripta Materialia, **162**: 286-291.

Submitted : 09/06/2019

Revised : 19/07/2019

Accepted : 23/07/2019